

# Role of Quantum Coherence in Kinetic Uncertainty Relations

Kacper Prech,<sup>1,\*</sup> Patrick P. Potts,<sup>1</sup> and Gabriel T. Landi<sup>2</sup>

<sup>1</sup>*Department of Physics and Swiss Nanoscience Institute,  
University of Basel, Klingelbergstrasse 82, 4056 Basel, Switzerland*

<sup>2</sup>*Department of Physics and Astronomy, University of Rochester, P.O. Box 270171 Rochester, NY, USA*

The kinetic uncertainty relation (KUR) bounds the signal-to-noise ratio of stochastic currents in terms of the number of transitions per unit time, known as the dynamical activity. This bound was derived in a classical context and can be violated in the quantum regime due to coherent effects. However, the precise connection between KUR violations and quantum coherence has so far remained elusive, despite significant investigation. In this Letter, we solve this problem by deriving a modified bound that exactly pinpoints how, and when, coherence might lead to KUR violations. Our bound is sensitive to the specific kind of unraveling of the quantum master equation. It, therefore, allows one to compare quantum jumps and quantum diffusion, and understand, in each case, how quantum coherence affects fluctuations. We illustrate our result on a double quantum dot, where the electron current is monitored either by electron jump detection or with continuous diffusive charge measurement.

*Introduction*—Superposition is one of the key features of quantum mechanics that distinguishes it from classical physics. While the most prominent consequences of quantum coherence are entanglement and nonlocality [1–3], it also has a profound effect on dynamical properties, such as the fluctuations of currents in open quantum systems [4–6], and thermodynamic quantities such as heat and work [7–21]. Crucially, since these fluctuations depend on two-time correlations [22], this effect is not necessarily related to the amount of coherence present in a quantum state, but rather to the dynamical generation and consumption of coherence in a process. However, the precise way in which this takes place remains poorly understood.

In classical systems, current fluctuations are constrained by a set of bounds, discovered over the last decade, and collectively known as thermokinetic uncertainty relations [23–36]. They provide lower bounds on the noise-to-signal ratio  $D/J^2$ , where  $J$  is the average current, and  $D$  (called the noise, scaled variance, or diffusion coefficient) quantifies its fluctuations. Two prominent classes of bounds are the thermodynamic uncertainty relation (TUR) [25, 26] and the kinetic uncertainty relation (KUR) [23, 24]. This Letter will focus on the latter, which reads

$$\frac{D}{J^2} \geq \frac{1}{A}, \quad (1)$$

where  $A$  is the average dynamical activity (“freneticity”) [37] and measures the average number of transitions per unit time in a stochastic system. The fact that the right-hand side depends on  $1/A$  means that high dynamical activities are required in order to decrease fluctuations. The bound, therefore, has a very practical implication in establishing the minimum activity required to achieve a certain precision. The TUR has an analogous form to the KUR, but the bound is given in terms of the average entropy production rate in place of the dynamical activity, which is a measure of irreversibility.

In the quantum domain, however, Eq. (1) can be violated. Several authors have worked to pinpoint the precise mechanisms responsible for these violations [4–6, 38–47]. While TUR violations received a considerable amount of attention, results for the KUR were first explored recently in [4]. It is noteworthy that quantum effects are not always beneficial for reducing fluctuations, and there are cases where it can actually be deleterious [40].

This, therefore, begs the question of when, and how, can coherence be used to improve the precision of stochastic currents? This led several authors to derive quantum extensions of the TUR and KUR [48–57]. These bounds are very useful in providing practical constraints. And they have also helped shed light on what new ingredients come into play when we move to the quantum domain. Unfortunately, they do not shed much light on the precise roles of coherence.

In this Letter we derive a new bound that holds for Markovian open quantum systems, in the presence of arbitrary quantum coherent effects. It replaces Eq. (1) with

$$\frac{D}{J^2} \geq \frac{(1 + \psi)^2}{A}, \quad (2)$$

where  $\psi \propto [\hat{H}, \hat{\rho}_{\text{ss}}]$  [c.f. Eq. (6)] is directly proportional to how much the steady-state density matrix  $\hat{\rho}_{\text{ss}}$  fails to commute with the system Hamiltonian  $\hat{H}$  (i.e., to the amount of energetic coherence present in the steady state). We refer to Eq. (2) as the  $\psi$ -KUR. A nearly identical bound also holds for the diffusive unraveling, with  $(1 + \psi) \rightarrow (1/2 + \psi)$ . In diffusive measurements, instead of directly detecting each monitored transition, their outputs are combined with strong reference currents, and their deviations are observed [58, 59]. For incoherent processes  $\psi = 0$ , and our result reduces to the classical KUR [Eq. (1)]. Conversely, for coherent processes, violations of Eq. (1) become possible when  $\psi \in [-2, 0]$ , while outside this interval violations are strictly not allowed.

This, therefore, unambiguously pinpoints energetic coherence as the fundamental ingredient required for KUR violations. The inequality in Eq. (2) also uncovers the special case  $\psi = -2$ , in which the original KUR holds, even though the system has coherence. To illustrate the significance of this special point, as well as the intuition behind Eq. (2), we carry out a detailed analysis of a double quantum dot (DQD) model [60].

*The  $\psi$ -KUR*—We consider an open quantum system with a density matrix  $\hat{\rho}_t$  that evolves in time according to the Lindblad master equation [61–64] ( $\hbar = 1$ )

$$\frac{d}{dt}\hat{\rho}_t = -i[\hat{H}, \hat{\rho}_t] + \sum_k D[\hat{L}_k]\hat{\rho}_t =: \mathcal{L}\hat{\rho}_t, \quad (3)$$

where  $\hat{H}$  is the Hamiltonian of the system,  $\hat{L}_k$  are Lindblad jump operators, and  $D[\hat{O}]\hat{\rho}_t := \hat{O}\hat{\rho}_t\hat{O}^\dagger - \frac{1}{2}\{\hat{O}^\dagger\hat{O}, \hat{\rho}_t\}$ . We assume the system has a unique steady state  $\mathcal{L}\hat{\rho}_{ss} = 0$ .

The derivation of Eq. (2) is done in the Appendix. Here we only make explicit the main quantities involved. Our bound concerns generic stochastic counting observables and integrated currents  $N(\tau)$ , whose definition depends on the unraveling in question (specified below). The average and scaled variance (noise) of the stochastic current  $I(\tau) = dN(\tau)/d\tau$  are given by

$$J = \frac{E[N(\tau)]}{\tau}, \quad D = \frac{\text{Var}[N(\tau)]}{\tau}, \quad (4)$$

where  $E[\cdot]$  denotes the expectation value and  $\text{Var}[\cdot]$  the variance. The dynamical activity reads [48, 49]

$$A = \sum_k \text{Tr}\{\hat{L}_k\hat{\rho}_{ss}\hat{L}_k^\dagger\} \quad (5)$$

and represents the average number of jumps per unit time in the steady state. In turn, the factor  $\psi$  in Eq. (2) is given by the expression

$$\psi = \frac{\text{Tr}\{\mathcal{J}\mathcal{L}^+\mathcal{H}\hat{\rho}_{ss}\}}{J}, \quad (6)$$

where  $\mathcal{H}\hat{\rho} := -i[\hat{H}, \hat{\rho}]$ ,  $\mathcal{L}^+$  is the Drazin inverse [65] of  $\mathcal{L}$  (see Supplemental Material [66] for details), and  $\mathcal{J}$  is the current superoperator, i.e.,  $J = \text{Tr}\{\mathcal{J}\hat{\rho}\}$ . We note that the superoperator  $\mathcal{H}$  describes the amount of steady-state energetic coherence, whereas the Drazin inverse depends on the relaxation rates, highlighting that  $\psi$  depends on the dynamics.

Crucially, since  $\psi$  depends on  $\mathcal{J}$ , our bound is sensitive to both the particular current measurement and the type of unraveling. For the jump unraveling, the current superoperator is given by

$$\mathcal{J}\hat{\rho} = \sum_k \nu_k \hat{L}_k \hat{\rho} \hat{L}_k^\dagger, \quad (7)$$

where  $\nu_k$  denotes the weight with which a jump  $\hat{L}_k$  changes the integrated current  $N(t)$  [22, 58]. Conversely, for the diffusive unraveling [22, 58]

$$\mathcal{J}_d\hat{\rho} = \sum_k \nu_k \left( e^{-i\phi_k} \hat{L}_k \hat{\rho} + \hat{\rho} \hat{L}_k^\dagger e^{i\phi_k} \right), \quad (8)$$

where  $\phi_k$  are arbitrary angles. In this case the bound Eq. (2) holds with the replacements  $(1 + \psi) \rightarrow (1/2 + \psi)$ ,  $\mathcal{J} \rightarrow \mathcal{J}_d$ , and  $J \rightarrow J_d$ .

Having introduced the quantum  $\psi$ -KUR [Eq. (2)], we compare it with a different, previously obtained bound [48]:

$$\frac{D}{J^2} \geq \frac{1}{A + \chi}, \quad (9)$$

which also applies in the steady state for the quantum jump unraveling of the Lindblad master equation [Eq. (3)]. For the diffusive unraveling, 1 is replaced by  $1/4$  in the numerator. Here  $\chi$  is a different coherence-dependent factor (see Supplemental Material [66] for the expression). However, as opposed to  $\psi$ , it does not concisely capture how much  $\hat{\rho}$  fails to commute with  $\hat{H}$ . Moreover, for a given system, the factor  $\chi$  is the same for all unravelings and current measurements, because it does not depend on the current superoperator  $\mathcal{J}$ , forfeiting a tailoring of the noise-to-signal bound to a particular current measurement. This is in contrast to  $\psi$ .

*Double quantum dot*—We illustrate the  $\psi$ -KUR (2) on a DQD model [60], where we find that  $\psi \in [-2, 0]$  allows for considerable violations of the classical KUR due to coherence when the noise  $D$  cannot be faithfully described by a classical model. The system consists of left (L) and right (R) spinless quantum dots, which are weakly coupled to their respective fermionic reservoirs. The Hamiltonian is

$$\hat{H} = \sum_{\ell=L,R} \epsilon \hat{c}_\ell^\dagger \hat{c}_\ell + g \left( \hat{c}_L^\dagger \hat{c}_R + \hat{c}_R^\dagger \hat{c}_L \right), \quad (10)$$

where  $\hat{c}_\ell$  ( $\hat{c}_\ell^\dagger$ ) are annihilation (creation) operators of an electron in dot  $\ell = L, R$ ,  $\epsilon$  is the occupation energy of each quantum dot, and  $g$  the coherent tunnel strength. The chemical potential, inverse temperature, and coupling strength to reservoir  $\ell$  are denoted by  $\mu_\ell$ ,  $\beta_\ell$ , and  $\gamma_\ell$ , respectively.

The Lindblad master equation governing the time evolution of the system is given by

$$\mathcal{L}\hat{\rho} = -i[\hat{H}, \hat{\rho}] + \sum_\ell \mathcal{L}_\ell \hat{\rho} + \frac{\Gamma}{2} D[\hat{c}_L^\dagger \hat{c}_L - \hat{c}_R^\dagger \hat{c}_R] \hat{\rho}, \quad (11)$$

where the last term denotes a dephasing in the local basis, with strength  $\Gamma$ , while

$$\mathcal{L}_\ell \hat{\rho} = \gamma_\ell \left( f_\ell D[\hat{c}_\ell^\dagger] + (1 - f_\ell) D[\hat{c}_\ell] \right) \hat{\rho} \quad (12)$$

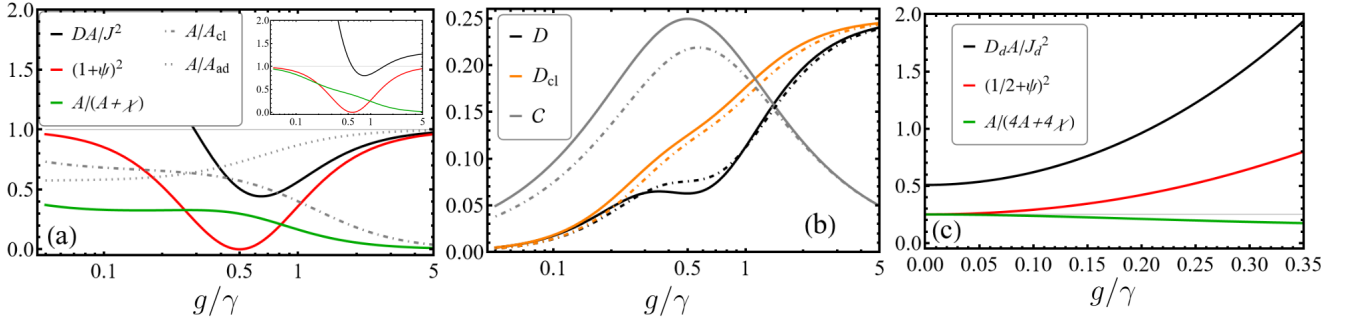


FIG. 1.  $\psi$ -KUR in the DQD. (a) Current fluctuations in the quantum jump unraveling as a function of  $g/\gamma$ , with  $\gamma = \gamma_L = \gamma_R$  and no dephasing ( $\Gamma = 0$ ): (black)  $DA/J^2$ ; (red)  $(1+\psi)^2$  [computed from Eq. (13)], which bounds the black curve according to Eq. (2); (green)  $A/(A+\chi)$  from Eq. (9); (dashed gray)  $A/A_{cl}$ ; (dotted gray)  $A/A_{ad}$ . Parameters:  $\beta_L \mu_L = -\beta_R \mu_R = 7$  and  $\epsilon = 0$ . The inset shows the same plots with dephasing rate  $\Gamma/\gamma = 0.3$ . (b) The noise  $D$  as a function of  $g/\gamma$  for the quantum (black) and classical (orange) models, as well as the  $l_1$  norm of coherence  $C$  (gray) obtained with Eq. (14). Solid lines correspond to the parameters of (a) (without dephasing) and dashed lines to those of the inset of (a) (with dephasing). (c) Same as (a) but for the diffusive measurement of the charge difference between the quantum dots. Parameters are the same as in (a), except  $\Gamma/\gamma = 1$ .

describes the coupling to reservoir  $\ell$ , with Fermi-Dirac occupation  $f_\ell := (\exp(\beta_\ell(\epsilon - \mu_\ell)) + 1)^{-1}$ .

For the quantum jump unraveling, we consider a net flow of electrons from the left reservoir through the system, which has the average current  $J = \gamma_L \text{Tr}\{f_L \hat{c}_L^\dagger \hat{\rho} \hat{c}_L - (1 - f_L) \hat{c}_L \hat{\rho} \hat{c}_L^\dagger\}$ . The analytical expression for  $\psi$  in this case reads

$$\psi = \frac{-2\gamma_L \gamma_R (\gamma_L + \gamma_R + 2\Gamma)}{4g^2 (\gamma_L + \gamma_R) + \gamma_L \gamma_R (\gamma_L + \gamma_R + 2\Gamma)} < 0, \quad (13)$$

which ranges between  $\psi = -2$  when  $g \rightarrow 0$  and  $\psi = 0$  when  $g \rightarrow \infty$ . It is, thus, always in the range  $(1+\psi)^2 < 1$  such that, for this model, the DQD coherence always allows for a reduced minimal activity to sustain a fixed noise-to-signal ratio. Fig. 1(a) compares  $DA/J^2$  with  $(1+\psi)^2$  as a function of  $g/\gamma$ . The bound is found to be tighter for large  $g/\gamma$ . Moreover, it is tighter than Eq. (9) for the majority of values  $g/\gamma$ , but not always.

The steady-state coherence, quantified by the  $l_1$  norm [67] in the occupation basis, is (see Supplemental Material [66])

$$C = \frac{2g|f_L - f_R|}{\gamma_L + \gamma_R + \Gamma} |\psi| \quad (14)$$

Thus, the range of coherent tunnel strength  $g$  where  $\psi$  predicts a significant contribution of coherence to the KUR violation corresponds to the peak of coherence.

Dephasing ( $\Gamma$ ) is found to be detrimental to loosening the KUR bound, and we find  $(1+\psi)^2 \rightarrow 1$  in the strong  $\Gamma$  limit consistently with our expectations for incoherent dynamics. A similar, anticipated effect of dephasing, which features in the inset of Fig. 1(a), is that  $DA/J^2$  obeys Eq. (1) in a much wider range of  $g/\gamma$ .

*Breakdown of the classical description*—To gain additional insights we ask whether the noise  $D$  can be captured by an effective classical model, where transport is

described by a Markovian rate equation

$$\frac{d}{dt} \vec{p} = W \vec{p}, \quad (15)$$

where  $W$  is a matrix of transition rates and  $\vec{p} = [p_0, p_L, p_R, p_D]$  is a vector of probabilities that the system is empty, occupied on the left, occupied on the right, or doubly occupied. The rates arising from the coupling to the environment are obtained from Eq. (12); for instance,  $W_{L0} = \gamma_L f_L$ . Conversely, the coherent tunneling is replaced by the rate

$$W_{LR} = W_{RL} = \frac{4g^2}{\gamma_L + \gamma_R + 2\Gamma}, \quad (16)$$

which can be obtained from perturbation theory [4, 5, 68] or by imposing that the two models should have the same average current.

Fig. 1(b) compares the noise in the classical and quantum models. While the classical model describes the average current in the entire range of  $g/\gamma$ , there is a discrepancy in the noise  $D$ , which appears precisely where the coherence in Eq. (14) has a peak. In this regime, the classical model fails to reproduce the reduction of the noise predicted by the quantum master equation. This coincides with the range where  $(1+\psi)^2 < 1$ , i.e., where the  $\psi$ -KUR in Eq. (2) differs from the KUR in Eq. (1).

While the classical model reproduces the noise for both small and large  $g/\gamma$ , these limits are quite different in nature. For large  $g$ , the Lindblad jumps provide the bottleneck for transport and, thus, determine the average current and the noise. Indeed, in this regime  $p_L - p_R \simeq 0$  can be adiabatically eliminated, and the classical model reduces to a three-state model  $\vec{p} = [p_0, p_L + p_R, p_D]$  (see Supplemental Material [66] for details). In this limit, coherence is suppressed and  $\psi = 0$ . In the limit of small

$g/\gamma$ , transport is dominated by the coherent tunneling, which now provides the bottleneck, but this tunneling can be captured by the perturbative rate  $W_{LR}$ . In this case, we obtain  $\psi \rightarrow -2$ , which also constitutes a classical limit where the  $\psi$ -KUR reduces to Eq. (1). As shown in the Appendix, since the current can be expressed as a series of conductances containing both perturbative rates and Lindblad jump rates, we find  $\psi \in [-2, 0]$ .

It is important to point out that the dynamical activity of the classical model differs from that of the quantum model given in Eq. (5). Indeed, the classical model implies the bound  $D/J^2 \geq 1/A_{\text{cl}}$  with the dynamical activity  $A_{\text{cl}} = A + (W_{LR} - \Gamma/2)(p_L + p_R)$  [see Fig. 1(a)]. The term proportional to  $\Gamma$  is subtracted, because dephasing jumps contribute to the dynamical activity of the quantum model but not in the classical rate equation. Nonetheless, for small  $\Gamma$ , in the regimes where the DQD behaves classically, the quantity  $A$  is the relevant quantity that bounds the signal-to-noise ratio according to Eq. (1). For small  $g/\gamma$  the contribution from  $W_{LR}$  is negligible, and  $A_{\text{cl}} \simeq A$ . For large  $g/\gamma$ , interdot transitions are very rapid but do not influence the noise. As mentioned above, the relevant classical dynamics may be described by a coarse-grained three-state model. The dynamical activity of this model,  $A_{\text{ad}}$ , tends to  $A$  for large  $g/\gamma$  [see Fig. 1(a)]. Therefore, in the regimes where  $D$  is captured by the classical model, the  $\psi$ -KUR in Eq. (2) provides the relevant bound for the signal-to-noise ratio. We note that, in contrast to the  $\psi$ -KUR, the KUR in Eq. (9) becomes very loose as  $g/\gamma$  becomes large as the denominator on the right-hand side approaches  $A_{\text{cl}}$ . We note that Eqs. (2) and (9) can be combined to obtain a tighter bound.

*Diffusive charge measurement*— We consider next the diffusive measurements of the charge difference between the dots, which can be implemented using a quantum point contact [22, 45, 69, 70]. The resulting diffusive current is  $J_d = \sqrt{2\Gamma} \text{Tr}\{(\hat{c}_L^\dagger \hat{c}_L - \hat{c}_R^\dagger \hat{c}_R) \hat{\rho}\}$ , where we assumed that all dephasing in Eq. (11) is due to the measurement. The  $\psi$ -KUR is illustrated in Fig. 1(c), where now

$$\psi = \frac{8g^2(\gamma_L + \gamma_R)}{4g^2(\gamma_L + \gamma_R) + \gamma_L\gamma_R(\gamma_L + \gamma_R + 2\Gamma)}. \quad (17)$$

In this case  $\psi > 0$  always, resulting in a tighter bound than the KUR [i.e., no violations of Eq. (1) are allowed]. One of the key features of the  $\psi$ -KUR is that it is unraveling dependent. For instance, we can contrast our result with the quantum bound in Eq. (9) (green line), which exhibits opposite behavior when compared to Eq. (2), thus representing a looser constraint on the noise-to-signal ratio. Interestingly, diffusive charge measurement is not the only example where we find  $\psi > 0$ . It happens also for the jump current, where we count only electrons entering the system from the left reservoir, which corresponds to the current  $J = \gamma_L f_L \text{Tr}\{\hat{c}_L^\dagger \hat{\rho} \hat{c}_L\}$  (see Supplemental Material [66]).

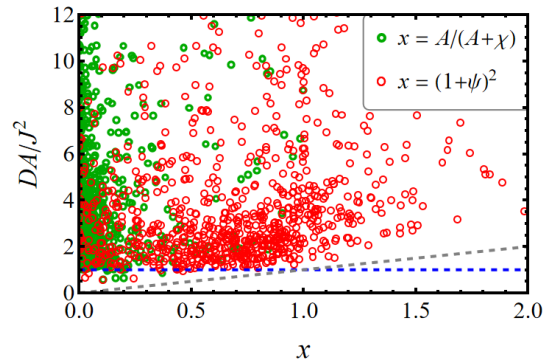


FIG. 2. A scatter plot of  $DA/J^2$  against  $(1 + \psi)^2$  (red circles) and  $A/(A + \chi)$  (green circles) for 1000 random networks of a five-level quantum system. Each transition  $|n\rangle \leftrightarrow |k\rangle$  is either coherently or dissipatively connected. Coherent tunneling strength  $g_{nk} = g_{kn}$  and jumping rates  $\gamma_{nk}$  are sampled from a uniform  $U[0, 3]$ , whereas  $\gamma_{kn} = \gamma_{nk} e^{-\sigma_{nk}}$ , with  $\sigma_{nk}$  sampled from  $U[3, 5]$ . The current is defined along a single edge with antisymmetric weights  $\pm 1$ . The gray dashed line represents  $x$ , i.e., the  $\psi$ -KUR bound in Eq. (2) for red circles and the bound in Eq. (9) for green circles. The blue dashed line is 1, i.e., the classical KUR bound in Eq. (1).

*Random network of states*— To illustrate the  $\psi$ -KUR in more general settings, we numerically investigate a five-level system, where each transition  $|n\rangle \leftrightarrow |k\rangle$  between the computational basis states is realized either by a coherent interaction  $g_{nk}|n\rangle\langle k|$  or jump operators  $\sqrt{\gamma_{nk}}|n\rangle\langle k|$  and  $\sqrt{\gamma_{kn}}|k\rangle\langle n|$ . Values of  $g_{nk} = g_{kn}$  and  $\gamma_{nk}$  are randomly sampled from a uniform distribution  $U[0, 3]$ , whereas  $\gamma_{kn} = \gamma_{nk} e^{-\sigma_{nk}}$ , with  $\sigma_{nk}$  sampled from  $U[3, 5]$  to ensure a strong bias. We consider an antisymmetric current for a single transition  $|0\rangle \leftrightarrow |1\rangle$ , meaning that  $\sqrt{\gamma_{10}}|1\rangle\langle 0|$  and  $\sqrt{\gamma_{01}}|0\rangle\langle 1|$  have weights 1 and  $-1$ , respectively, whereas all other jumps are not counted toward the current.

The red circles in Fig. 2 show  $DA/J^2$  vs  $(1 + \psi)^2$  for 1000 randomly sampled networks. These points illustrate that the factor  $\psi$  may be both positive and negative, and that the  $\psi$ -KUR provides a relevant bound also for more complex systems. The green circles show  $DA/J^2$  vs  $A/(A + \chi)$  for the same network. It is noteworthy that many green circles fall close to  $x = 0$ , where Eq. (9) reduces to the trivial bound  $DA/J^2 \geq 0$ .

*Conclusions and outlook*—We derived an unraveling-dependent quantum KUR that holds for Markovian open quantum systems in the steady state, and includes a factor ( $\psi$ ) that captures the effect of energetic coherence in the density matrix. This bound pinpoints precisely how coherence may or may not allow for violations of the classical KUR. The physical significance of our results is substantiated by illustrating the KUR and the meaning of  $\psi$  on the DQD with two different unravelings corresponding to different measurements. Interesting future questions include deriving thermokinetic uncertainty

relations under strong system-environment couplings or for a unitary description of system and environment, investigating the transient regime [49, 71, 72], extending the results to the first passage times [49, 73], exploring the implications of our findings on the precision of clocks [52, 74, 75], and generalizing a newly established clock uncertainty relation [76, 77], which constitutes a generally tighter bound than the classical KUR with the average residual time in place of the dynamical activity, to the quantum regime. Since there is a growing interest in current fluctuations in non-Markovian settings [78, 79], with a potential development of a theory of unravelings in non-Markovian master equations [80], our methods could be useful to find similar bounds on the signal-to-noise ratio.

*Acknowledgements*—P.P.P. and K.P. acknowledge funding from the Swiss National Science Foundation (Excellence Professorial Fellowship PCEFP2.194268).

### Appendix: Derivation of $\psi$ -KUR [Eq. (2)]

To derive the  $\psi$ -KUR given in Eq. (2), we consider the following deformation of the jump operators in the Lindblad master equation [Eq. (3)]:  $\hat{L}_k \rightarrow \hat{L}_{k,\theta} := \sqrt{1+\theta}\hat{L}_k$ . This results in the modified Lindblad master equation

$$\frac{d}{dt}\hat{\rho}_t = -i[\hat{H}, \hat{\rho}_t] + (1+\theta) \sum_k D[\hat{L}_k]\hat{\rho} =: \mathcal{L}_\theta \hat{\rho}_t, \quad (18)$$

such that we recover the original master equation when  $\theta \rightarrow 0$ . Contrary to the method used to derive Eq. (9), here the deformation is only in the jump operators. It, therefore, does not amount to a homogeneous scaling of time. We use a generalized quantum Cramér-Rao bound [81, 82]

$$\text{Var}_\theta[N(\tau)]_{\theta=0} \geq \frac{(\partial_\theta \text{E}_\theta[N(\tau)]_{\theta=0})^2}{\mathcal{I}(\theta \rightarrow 0)}, \quad (19)$$

where  $\text{E}_\theta[N(\tau)]$  and  $\text{Var}_\theta[N(\tau)]$  denote the expectation value and the variance of  $N(\tau)$  corresponding to the distorted dynamics [Eq. (18)], and  $\mathcal{I}(\theta)$  is the quantum Fisher information (QFI) of the parameter  $\theta$ . In Eq. (19),  $N(\tau)$  plays the role of an estimator for the parameter  $\theta$ . While it may not be a good estimator (it is generally biased), it nevertheless is a possible estimator and, thus, obeys the Cramér-Rao bound. While Eq. (19) holds universally, analytically computing all expressions therein is often not straightforward, as evidenced by this Letter. Similarly, finding measurements that saturate it is highly nontrivial.

Using the formalism of Ref. [83] to compute the QFI of continuously monitored open quantum systems, we find

$$\mathcal{I}(\theta \rightarrow 0) = \tau A. \quad (20)$$

The expectation value of the time-integrated current is given by

$$\text{E}_\theta[N(\tau)] = \begin{cases} (1+\theta) \int_0^\tau dt \text{Tr}\{\mathcal{J} e^{\mathcal{L}_\theta t} \hat{\rho}\} & (\text{jump current}) \\ \sqrt{1+\theta} \int_0^\tau dt \text{Tr}\{\mathcal{J} e^{\mathcal{L}_\theta t} \hat{\rho}\} & (\text{diffusive current}). \end{cases} \quad (21)$$

Due to a different prefactor, we obtain two expressions for its partial derivative with respect to  $\theta$ :

$$\partial_\theta \text{E}_\theta[N(\tau)]_{\theta=0} = \begin{cases} J\tau(1+\psi) & (\text{jump current}) \\ J\tau(\frac{1}{2}+\psi) & (\text{diffusive current}) \end{cases}. \quad (22)$$

Using the relation  $\text{Var}_\theta[N(\tau)]_{\theta=0} = D\tau$  and inserting Eqs. (20) and (22) into the quantum Cramér-Rao bound [Eq. (19)] leads to our  $\psi$ -KUR [Eq. (2)]. See Supplemental Material [66] for a derivation of Eqs. (20) and (22).

The classical KUR [Eq. (1)] can be recovered in the limit of incoherent dynamics as a result of  $[\hat{H}, \hat{\rho}] = 0$ , implying  $\psi = 0$ . For the DQD, this is what happens in the limit  $g \rightarrow \infty$ . As discussed in the main text, we may also recover  $(1+\psi)^2 = 1$  when  $\psi = -2$ , which happens for the DQD in the limit  $g \rightarrow 0$  where both  $[\hat{H}, \hat{\rho}]$  as well as  $J$  tend to zero, c.f. Eq. (13). This observation may be understood by considering the rates in the classical model. In the limit of large  $g$ , the couplings to the bath become the bottleneck that dominates transport, and the current reduces to  $J = \gamma_L \gamma_R (f_L - f_R) / (\gamma_L + \gamma_R)$ . Under the rescaling in Eq. (18),  $\text{E}_\theta[N(\tau)] = J\tau(1+\theta)$ , which results in  $\psi = 0$  from Eq. (22). In contrast, in the limit of small  $g$ , interdot tunneling with rate  $W_{LR}$  provides the bottleneck and the current reduces to  $J = W_{LR}(f_L - f_R)$ . Since  $W_{LR}$  is inversely proportional to the Lindblad jump rates, the rescaled integrated current reduces to  $\text{E}_\theta[N(\tau)] = J\tau/(1+\theta) \simeq J\tau(1-\theta)$  for small  $\theta$ , which results in  $\psi = -2$ . For arbitrary interdot couplings, the current can be written as a series of conductances

$$J = (\gamma_L^{-1} + \gamma_R^{-1} + W_{LR}^{-1})^{-1}(f_L - f_R). \quad (23)$$

The rescaled current then reads, for small  $\theta$ ,

$$\text{E}_\theta[N(\tau)] = J\tau \left( 1 + \theta \frac{W_{LR}(\gamma_L + \gamma_R) - \gamma_L \gamma_R}{W_{LR}(\gamma_L + \gamma_R) + \gamma_L \gamma_R} \right), \quad (24)$$

which imposes in  $-2 \leq \psi \leq 0$ . As we detail in Supplemental Material [66], the same restrictions for  $\psi$  hold whenever the current can be written as a series of conductances including both perturbative rates as well as Lindblad jump rates.

It is interesting to examine Eqs. (2) and (9) as a quantum Cramér-Rao bound, c.f. Eq. (19). In Eq. (2), the quantum correction  $\psi$  arises from the numerator, i.e., the bias of the estimator. The bound becomes trivial (i.e., the right-hand side vanishes) when the estimator does not depend on  $\theta$ , which happens for  $\psi = -1$  [c.f. Eq. (22)]. In

this regime, where coherence plays a strong role, we can, thus, not expect our bound to be tight, as the fluctuations generally remain finite even when they do not contain information on  $\theta$ . In contrast, the quantum correction  $\chi$  in Eq. (9) arises from the quantum Fisher information, i.e., the denominator in Eq. (19) [48]. The bound becomes loose when there is a large amount of information on  $\theta$  in the output of the system. This generally happens when the system hosts fast processes, which allow for estimating time precisely, since in Ref. [48],  $\theta$  corresponds to a rescaling of time. This explains why Eq. (9) becomes loose for large  $g$  in Fig. 1.

---

\* kacper.prech@unibas.ch

- [1] A. Streltsov, G. Adesso, and M. B. Plenio, Colloquium: Quantum coherence as a resource, *Rev. Mod. Phys.* **89**, 041003 (2017).
- [2] R. Horodecki, P. Horodecki, M. Horodecki, and K. Horodecki, Quantum entanglement, *Rev. Mod. Phys.* **81**, 865 (2009).
- [3] N. Brunner, D. Cavalcanti, S. Pironio, V. Scarani, and S. Wehner, Bell nonlocality, *Rev. Mod. Phys.* **86**, 419 (2014).
- [4] K. Prech, P. Johansson, E. Nyholm, G. T. Landi, C. Verdozzi, P. Samuelsson, and P. P. Potts, Entanglement and thermokinetic uncertainty relations in coherent mesoscopic transport, *Phys. Rev. Res.* **5**, 023155 (2023).
- [5] G. Kießlich, P. Samuelsson, A. Wacker, and E. Schöll, Counting statistics and decoherence in coupled quantum dots, *Phys. Rev. B* **73**, 033312 (2006).
- [6] K. Ptaszyński, Coherence-enhanced constancy of a quantum thermoelectric generator, *Phys. Rev. B* **98**, 085425 (2018).
- [7] C. L. Latune, I. Sinayskiy, and F. Petruccione, Negative contributions to entropy production induced by quantum coherences, *Phys. Rev. A* **102**, 042220 (2020).
- [8] M. Scandi, H. J. D. Miller, J. Anders, and M. Perarnau-Llobet, Quantum work statistics close to equilibrium, *Phys. Rev. Res.* **2**, 023377 (2020).
- [9] H. Tajima and K. Funo, Superconducting-like heat current: Effective cancellation of current-dissipation trade-off by quantum coherence, *Phys. Rev. Lett.* **127**, 190604 (2021).
- [10] G. Francica, J. Goold, and F. Plastina, Role of coherence in the nonequilibrium thermodynamics of quantum systems, *Phys. Rev. E* **99**, 042105 (2019).
- [11] J. P. Santos, L. C. Céleri, G. T. Landi, and M. Paternostro, The role of quantum coherence in non-equilibrium entropy production, *Npj Quantum Inf.* **5**, 23 (2019).
- [12] G. T. Landi and M. Paternostro, Irreversible entropy production: From classical to quantum, *Rev. Mod. Phys.* **93**, 035008 (2021).
- [13] F. Rodrigues and E. Lutz, Nonequilibrium thermodynamics of quantum coherence beyond linear response, *Commun. Phys.* **7** (2024).
- [14] J. Kurchan, A quantum fluctuation theorem, *arXiv:cond-mat/0007360*.
- [15] H. Tasaki, Jarzynski relations for quantum systems and some applications, *arXiv:cond-mat/0009244*.
- [16] P. Talkner, E. Lutz, and P. Hänggi, Fluctuation theorems: Work is not an observable, *Phys. Rev. E* **75**, 050102(R) (2007).
- [17] M. Esposito, U. Harbola, and S. Mukamel, Nonequilibrium fluctuations, fluctuation theorems, and counting statistics in quantum systems, *Rev. Mod. Phys.* **81**, 1665 (2009).
- [18] M. Campisi, P. Hänggi, and P. Talkner, Colloquium: Quantum fluctuation relations: Foundations and applications, *Rev. Mod. Phys.* **83**, 771 (2011).
- [19] G. Manzano, J. M. Horowitz, and J. M. R. Parrondo, Quantum fluctuation theorems for arbitrary environments: Adiabatic and nonadiabatic entropy production, *Phys. Rev. X* **8**, 031037 (2018).
- [20] K. Prech and P. P. Potts, Quantum fluctuation theorem for arbitrary measurement and feedback schemes, *Phys. Rev. Lett.* **133**, 140401 (2024).
- [21] T. Yada, N. Yoshioka, and T. Sagawa, Quantum fluctuation theorem under quantum jumps with continuous measurement and feedback, *Phys. Rev. Lett.* **128**, 170601 (2022).
- [22] G. T. Landi, M. J. Kewming, M. T. Mitchison, and P. P. Potts, Current fluctuations in open quantum systems: Bridging the gap between quantum continuous measurements and full counting statistics, *PRX Quantum* **5**, 020201 (2024).
- [23] I. D. Terlizzi and M. Baiesi, Kinetic uncertainty relation, *J. Phys. A* **52**, 02LT03 (2018).
- [24] J. P. Garrahan, Simple bounds on fluctuations and uncertainty relations for first-passage times of counting observables, *Phys. Rev. E* **95**, 032134 (2017).
- [25] T. R. Gingrich, J. M. Horowitz, N. Perunov, and J. L. England, Dissipation bounds all steady-state current fluctuations, *Phys. Rev. Lett.* **116**, 120601 (2016).
- [26] A. C. Barato and U. Seifert, Thermodynamic uncertainty relation for biomolecular processes, *Phys. Rev. Lett.* **114**, 158101 (2015).
- [27] J. M. Horowitz and T. R. Gingrich, Thermodynamic uncertainty relations constrain non-equilibrium fluctuations, *Nat. Phys.* **16**, 15 (2020).
- [28] P. P. Potts and P. Samuelsson, Thermodynamic uncertainty relations including measurement and feedback, *Phys. Rev. E* **100**, 052137 (2019).
- [29] K. Macieszczak, K. Brandner, and J. P. Garrahan, Unified thermodynamic uncertainty relations in linear response, *Phys. Rev. Lett.* **121**, 130601 (2018).
- [30] P. Pietzonka, F. Ritort, and U. Seifert, Finite-time generalization of the thermodynamic uncertainty relation, *Phys. Rev. E* **96**, 012101 (2017).
- [31] J. M. Horowitz and T. R. Gingrich, Proof of the finite-time thermodynamic uncertainty relation for steady-state currents, *Phys. Rev. E* **96**, 020103(R) (2017).
- [32] T. Koyuk and U. Seifert, Thermodynamic uncertainty relation for time-dependent driving, *Phys. Rev. Lett.* **125**, 260604 (2020).
- [33] V. T. Vo, T. V. Vu, and Y. Hasegawa, Unified thermodynamic-kinetic uncertainty relation, *J. Phys. A* **55**, 405004 (2022).
- [34] K. Liu, Z. Gong, and M. Ueda, Thermodynamic uncertainty relation for arbitrary initial states, *Phys. Rev. Lett.* **125**, 140602 (2020).
- [35] Y. Hasegawa and T. Van Vu, Uncertainty relations in stochastic processes: An information inequality approach, *Phys. Rev. E* **99**, 062126 (2019).

- [36] A. M. Timpanaro, G. Guarnieri, J. Goold, and G. T. Landi, Thermodynamic uncertainty relations from exchange fluctuation theorems, *Phys. Rev. Lett.* **123**, 090604 (2019).
- [37] C. Maes, Frenesy: Time-symmetric dynamical activity in nonequilibria, *Phys. Rep.* **850**, 1 (2020), frenesy: time-symmetric dynamical activity in nonequilibria.
- [38] B. K. Agarwalla and D. Segal, Assessing the validity of the thermodynamic uncertainty relation in quantum systems, *Phys. Rev. B* **98**, 155438 (2018).
- [39] A. A. S. Kalaei, A. Wacker, and P. P. Potts, Violating the thermodynamic uncertainty relation in the three-level maser, *Phys. Rev. E* **104**, L012103 (2021).
- [40] A. Rignon-Bret, G. Guarnieri, J. Goold, and M. T. Mitchison, Thermodynamics of precision in quantum nanomachines, *Phys. Rev. E* **103**, 012133 (2021).
- [41] J. Liu and D. Segal, Coherences and the thermodynamic uncertainty relation: Insights from quantum absorption refrigerators, *Phys. Rev. E* **103**, 032138 (2021).
- [42] M. Gerry and D. Segal, Absence and recovery of cost-precision tradeoff relations in quantum transport, *Phys. Rev. B* **105**, 155401 (2022).
- [43] M. Gerry and D. Segal, Full counting statistics and coherences: Fluctuation symmetry in heat transport with the unified quantum master equation, *Phys. Rev. E* **107**, 054115 (2023).
- [44] M. Janovitch, M. Brunelli, and P. P. Potts, Wave-particle duality in a quantum heat engine, *Phys. Rev. Res.* **5**, L042007 (2023).
- [45] L. P. Bettmann, M. J. Kewming, and J. Goold, Thermodynamics of a continuously monitored double-quantum-dot heat engine in the repeated interactions framework, *Phys. Rev. E* **107**, 044102 (2023).
- [46] L. M. Cangemi, V. Cataudella, G. Benenti, M. Sasseti, and G. De Filippis, Violation of thermodynamics uncertainty relations in a periodically driven work-to-work converter from weak to strong dissipation, *Phys. Rev. B* **102**, 165418 (2020).
- [47] P. Menczel, E. Loisa, K. Brandner, and C. Flindt, Thermodynamic uncertainty relations for coherently driven open quantum systems, *J. Phys. A* **54**, 314002 (2021).
- [48] Y. Hasegawa, Quantum thermodynamic uncertainty relation for continuous measurement, *Phys. Rev. Lett.* **125**, 050601 (2020).
- [49] T. Van Vu and K. Saito, Thermodynamics of precision in Markovian open quantum dynamics, *Phys. Rev. Lett.* **128**, 140602 (2022).
- [50] G. Guarnieri, G. T. Landi, S. R. Clark, and J. Goold, Thermodynamics of precision in quantum nonequilibrium steady states, *Phys. Rev. Res.* **1**, 033021 (2019).
- [51] F. Carollo, R. L. Jack, and J. P. Garrahan, Unraveling the large deviation statistics of Markovian open quantum systems, *Phys. Rev. Lett.* **122**, 130605 (2019).
- [52] P. Erker, M. T. Mitchison, R. Silva, M. P. Woods, N. Brunner, and M. Huber, Autonomous quantum clocks: Does thermodynamics limit our ability to measure time?, *Phys. Rev. X* **7**, 031022 (2017).
- [53] Y. Hasegawa, Thermodynamic uncertainty relation for general open quantum systems, *Phys. Rev. Lett.* **126**, 010602 (2021).
- [54] Y. Hasegawa, Irreversibility, Loschmidt echo, and thermodynamic uncertainty relation, *Phys. Rev. Lett.* **127**, 240602 (2021).
- [55] H. J. D. Miller, M. H. Mohammady, M. Perarnau-Llobet, and G. Guarnieri, Thermodynamic uncertainty relation in slowly driven quantum heat engines, *Phys. Rev. Lett.* **126**, 210603 (2021).
- [56] Y. Hasegawa, Thermodynamic uncertainty relation for quantum first-passage processes, *Phys. Rev. E* **105**, 044127 (2022).
- [57] Y. Hasegawa, Quantum thermodynamic uncertainty relation under feedback control, arXiv:2312.07407.
- [58] H. Carmichael, An open systems approach to quantum optics, *Lect. Notes in Phys. Monogr.* **18**, 10.1007/978-3-540-47620-7 (1993).
- [59] K. Jacobs, *Quantum Measurement Theory and its Applications* (Cambridge University Press, Cambridge, England, 2014).
- [60] W. G. van der Wiel, S. De Franceschi, J. M. Elzerman, T. Fujisawa, S. Tarucha, and L. P. Kouwenhoven, Electron transport through double quantum dots, *Rev. Mod. Phys.* **75**, 1 (2002).
- [61] H.-P. Breuer and F. Petruccione, *The theory of open quantum systems* (Oxford University Press, Oxford, England, 2003).
- [62] P. P. Potts, A. A. S. Kalaei, and A. Wacker, A thermodynamically consistent markovian master equation beyond the secular approximation, *New J. Phys.* **23**, 123013 (2021).
- [63] M. B. Plenio and P. L. Knight, The quantum-jump approach to dissipative dynamics in quantum optics, *Rev. Mod. Phys.* **70**, 101 (1998).
- [64] G. Schaller, *Open Quantum Systems Far from Equilibrium*, Vol. 881 (Springer, Cham, 2013).
- [65] D. Mandal and C. Jarzynski, Analysis of slow transitions between nonequilibrium steady states, *J. Stat. Mech.* **2016**, 063204.
- [66] See supplemental material for details of derivation of  $\psi$ -kur, the expression for  $\chi$ , detailed calculations for the double quantum dot example, specifics of the scatter plot, and an additional example of a coherently driven qubit.
- [67] T. Baumgratz, M. Cramer, and M. B. Plenio, Quantifying coherence, *Phys. Rev. Lett.* **113**, 140401 (2014).
- [68] M. T. Mitchison, M. P. Woods, J. Prior, and M. Huber, Coherence-assisted single-shot cooling by quantum absorption refrigerators, *New J. Phys.* **17**, 115013 (2015).
- [69] H.-S. Goan, G. J. Milburn, H. M. Wiseman, and H. Bi Sun, Continuous quantum measurement of two coupled quantum dots using a point contact: A quantum trajectory approach, *Phys. Rev. B* **63**, 125326 (2001).
- [70] S. A. Gurvitz, Measurements with a noninvasive detector and dephasing mechanism, *Phys. Rev. B* **56**, 15215 (1997).
- [71] G. Blasi, S. Khandelwal, and G. Haack, Exact finite-time correlation functions for multiterminal setups: Connecting theoretical frameworks for quantum transport and thermodynamics, *Phys. Rev. Res.* **6**, 043091 (2024).
- [72] J. Bourgeois, G. Blasi, S. Khandelwal, and G. Haack, Finite-time dynamics of an entanglement engine: Current, fluctuations and kinetic uncertainty relations, *Entropy* **26**, 10.3390/e26060497 (2024).
- [73] M. J. Kewming, A. Kiely, S. Campbell, and G. T. Landi, First passage times for continuous quantum measurement currents, *Phys. Rev. A* **109**, L050202 (2024).
- [74] F. Meier, E. Schwarzthans, P. Erker, and M. Huber, Fundamental accuracy-resolution trade-off for timekeeping devices, *Phys. Rev. Lett.* **131**, 220201 (2023).
- [75] O. Culhane, M. J. Kewming, A. Silva, J. Goold, and

- M. T. Mitchison, Powering an autonomous clock with quantum electromechanics, *New J. Phys.* **26**, 023047 (2024).
- [76] K. Prech, G. T. Landi, F. Meier, N. Nurgalieva, P. P. Potts, R. Silva, and M. T. Mitchison, Optimal time estimation and the clock uncertainty relation for stochastic processes, arXiv:2406.19450.
- [77] K. Macieszczak, Ultimate kinetic uncertainty relation and optimal performance of stochastic clocks, arXiv:2407.09839.
- [78] M. Brenes, G. Guarnieri, A. Purkayastha, J. Eisert, D. Segal, and G. Landi, Particle current statistics in driven mesoscale conductors, *Phys. Rev. B* **108**, L081119 (2023).
- [79] L. P. Bettmann, M. J. Kewming, G. T. Landi, J. Goold, and M. T. Mitchison, Quantum stochastic thermodynamics in the mesoscopic-leads formulation, arXiv:2404.06426.
- [80] X. Li, S.-X. Lyu, Y. Wang, R.-X. Xu, X. Zheng, and Y. J. Yan, Toward quantum simulation of non-Markovian open quantum dynamics: A universal and compact theory, *Phys. Rev. A* **110**, 032620 (2024).
- [81] C. W. Helstrom, Quantum detection and estimation theory, *J. Stat. Phys.* **1**, 231 (1969).
- [82] M. Hotta and M. Ozawa, Quantum estimation by local observables, *Phys. Rev. A* **70**, 022327 (2004).
- [83] S. Gammelmark and K. Mølmer, Fisher information and the quantum Cramér-Rao sensitivity limit of continuous measurements, *Phys. Rev. Lett.* **112**, 170401 (2014).
-



# Supplemental Material: Role of Quantum Coherence in Kinetic Uncertainty Relations

Kacper Prech<sup>1,\*</sup>, Patrick P. Potts<sup>1</sup>, and Gabriel T. Landi<sup>2</sup>

<sup>1</sup>*Department of Physics and Swiss Nanoscience Institute, University of Basel, Klingelbergstrasse 82, 4056 Basel, Switzerland*

<sup>2</sup>*Department of Physics and Astronomy, University of Rochester, P.O. Box 270171 Rochester, NY, USA*

\* kacper.prech@unibas.ch

In Sec. I we present the derivation of the quantum KUR, Eq. (2) in the main text. In Sec. II we discuss a restriction on  $\psi$  when the corresponding current can be expressed as a series of conductances. In Sec. III we state the KUR of Ref. [48], Eq. (9) in the main text. In Sec. IV we provide details about the Drazin inverse and how to compute it, provide useful relations about vectorization of quantum operators, and explain how to compute the noise  $D$ . Details of the double quantum dot are presented in Sec. V. The classical model, including the rate equation and the adiabatic elimination for large  $g$ , are discussed in Sec. VI. In Sec. VII we give details about the example with the random network of states. Lastly, in Sec. VIII, we introduce and investigate a coherently driven qubit, an additional, further example illustrating our results.

## I. Derivation of the quantum KUR

In this section, we present a derivation of Eqs. (20) and (22) in the main text.

### Calculation of the QFI $\mathcal{I}(\theta)$

In order to derive Eq. (20) in the main text, the QFI is computed using the result of Gammelmark and Mølmer [83]:

$$\mathcal{I}(\theta) = 4\tau \sum_k \text{Tr}\{(\partial_\theta \hat{L}_{k,\theta})^\dagger (\partial_\theta \hat{L}_{k,\theta}) \hat{\rho}_{ss}\} - 4\tau \left( \text{Tr}\{\mathcal{L}_L \mathcal{L}^+ \mathcal{L}_R \hat{\rho}_{ss}\} + \text{Tr}\{\mathcal{L}_R \mathcal{L}^+ \mathcal{L}_L \hat{\rho}_{ss}\} \right), \quad (\text{S1})$$

where

$$\begin{aligned} \mathcal{L}_L \hat{\rho} &= -i\partial_\theta \hat{H} \hat{\rho} - \frac{1}{2} \sum_k \partial_\theta (\hat{L}_{k,\theta}^\dagger \hat{L}_{k,\theta}) \hat{\rho} + \sum_k (\partial_\theta \hat{L}_{k,\theta}) \hat{\rho} \hat{L}_{k,\theta}^\dagger, \\ \mathcal{L}_R \hat{\rho} &= i\hat{\rho} \partial_\theta \hat{H} - \frac{1}{2} \sum_k \hat{\rho} \partial_\theta (\hat{L}_{k,\theta}^\dagger \hat{L}_{k,\theta}) + \sum_k \hat{L}_{k,\theta} \hat{\rho} (\partial_\theta \hat{L}_{k,\theta})^\dagger. \end{aligned} \quad (\text{S2})$$

In the parametrization considered in Eq. (18) in the main text, only jump operators,  $L_{k,\theta} = \sqrt{1+\theta} L_k$ , are dependent on  $\theta$ . Therefore, in the limit  $\theta \rightarrow 0$ , the superoperators  $\mathcal{L}_{L,R}$  reduce to

$$\begin{aligned} \mathcal{L}_L \hat{\rho} &= \frac{1}{2} \sum_k \left( \hat{L}_k \hat{\rho} \hat{L}_k^\dagger - \hat{L}_k^\dagger \hat{L}_k \hat{\rho} \right), \\ \mathcal{L}_R \hat{\rho} &= \frac{1}{2} \sum_k \left( \hat{L}_k \hat{\rho} \hat{L}_k^\dagger - \hat{\rho} \hat{L}_k^\dagger \hat{L}_k \right). \end{aligned} \quad (\text{S3})$$

One can observe, however, that these operators are traceless,  $\text{Tr}\{\mathcal{L}_{L,R} \hat{\rho}\} = 0$ . Therefore, the last two terms in Eq. (S1) vanish, and in the limit  $\theta \rightarrow 0$ , the QFI reduces to

$$\mathcal{I}(\theta \rightarrow 0) = \tau \sum_k \text{Tr}\{L_k^\dagger L_k \hat{\rho}_{ss}\} = \tau A, \quad (\text{S4})$$

where  $A$  is the dynamical activity, see Eq. (5) in the main text.

### Calculation of $\partial_\theta \mathbb{E}_\theta[N(\tau)]$

Here we show how to obtain Eq. (22) in the main text, starting from the jump current. For  $\theta = 0$ , the average of  $N(\tau)$  is given by

$$\begin{aligned} \mathbb{E}[N(\tau)] &= \int_0^\tau \mathbb{E}[dN_t] = \sum_k \int_0^\tau dt \nu_k \text{Tr}\{\hat{L}_k \hat{\rho}_t \hat{L}_k^\dagger\} \\ &= \sum_k \int_0^\tau dt \nu_k \text{Tr}\{\hat{L}_k^\dagger \hat{L}_k e^{\mathcal{L}t} \hat{\rho}_0\}, \end{aligned} \quad (\text{S5})$$

where the density matrix explicitly includes a time dependence. The corresponding quantity in the deformed dynamics is given by

$$\mathbb{E}_\theta[N(\tau)] = (1 + \theta) \sum_k \int_0^\tau dt \nu_k \text{Tr}\{\hat{L}_k^\dagger \hat{L}_k e^{\mathcal{L}_\theta t} \hat{\rho}_0\}, \quad (\text{S6})$$

with  $\hat{\rho}_0$  being the initial state. Since  $\theta$  appears both in the prefactor and in the  $e^{\mathcal{L}_\theta t}$  term, we find

$$\begin{aligned} \partial_\theta \mathbb{E}_\theta[N(\tau)] &= \sum_k \int_0^\tau dt \nu_k \text{Tr}\{\hat{L}_k^\dagger \hat{L}_k e^{\mathcal{L}_\theta t} \hat{\rho}_0\} \\ &\quad + (1 + \theta) \sum_k \int_0^\tau dt \nu_k \text{Tr}\{\hat{L}_k^\dagger \hat{L}_k (\partial_\theta e^{\mathcal{L}_\theta t}) \hat{\rho}_0\}. \end{aligned} \quad (\text{S7})$$

Since this expression is written in terms of the time evolution from the initial state, there is no  $\theta$  dependence in  $\hat{\rho}_0$ . Recall that we are only interested in the limit  $\theta \rightarrow 0$ . Thus, for instance, the first term, taking  $\hat{\rho}_0$  to be the steady state, simplifies to

$$\lim_{\theta \rightarrow 0} \sum_k \int_0^\tau dt \nu_k \text{Tr}\{\hat{L}_k^\dagger \hat{L}_k e^{\mathcal{L}_\theta t} \hat{\rho}_0\} = \tau J, \quad (\text{S8})$$

where  $J$  is the average current, see Eq. (4) in the main text. To simplify the second term in Eq. (S7), we apply a Dyson series expansion to  $\mathcal{L}_\theta = \mathcal{L} + \theta \mathcal{D}$ , which leads to

$$e^{\mathcal{L}_\theta t} = e^{\mathcal{L}t} + \theta \int_0^t dt_1 e^{\mathcal{L}(t-t_1)} \mathcal{D} e^{\mathcal{L}t_1} + \mathcal{O}(\theta^2). \quad (\text{S9})$$

Thus, to leading order, we have

$$\partial_\theta e^{\mathcal{L}_\theta t} = \int_0^t dt_1 e^{\mathcal{L}(t-t_1)} \mathcal{D} e^{\mathcal{L}t_1} + \mathcal{O}(\theta). \quad (\text{S10})$$

Inserting this expression into Eq. (S7) results in

$$\partial_\theta \mathbb{E}_\theta[N(\tau)]_{\theta=0} = \tau J + \sum_k \nu_k \int_0^\tau dt \int_0^t dt_1 \text{Tr}\{\hat{L}_k^\dagger \hat{L}_k e^{\mathcal{L}(t-t_1)} \mathcal{D} e^{\mathcal{L}t_1} \hat{\rho}_0\}. \quad (\text{S11})$$

Since  $\hat{\rho}_0$  is the steady state, we have  $e^{\mathcal{L}t_1} \hat{\rho}_0 = \hat{\rho}_0$ , leading to

$$\partial_\theta \mathbb{E}_\theta[N(\tau)]_{\theta=0} = \tau J + \sum_k \nu_k \int_0^\tau dt \int_0^t dt_1 \text{Tr}\{\hat{L}_k^\dagger \hat{L}_k e^{\mathcal{L}(t-t_1)} \mathcal{D} \hat{\rho}_0\}. \quad (\text{S12})$$

To evaluate the second term on the right-hand-side of the equation above, we switch to a vectorized notation. The trace and the steady state are the left and right eigenvectors of the Liouvillian's zero eigenvalue:

$$\langle 1 | \mathcal{L} = 0 \quad \text{and} \quad \mathcal{L} | \rho \rangle = 0, \quad (\text{S13})$$

respectively. We assume the steady state is unique and the Liouvillian is diagonalizable. The latter is not necessary, but does simplify what follows. The remaining eigenvalue and eigenvector pairs will be denoted as

$$\mathcal{L}|x_j\rangle = \lambda_j|x_j\rangle \quad \text{and} \quad \langle y_j|\mathcal{L} = \lambda_j\langle y_j|. \quad (\text{S14})$$

It is also assumed that the system is stable, which implies that  $\text{Re}(\lambda_j) < 0$ . Moreover, orthogonality implies that the eigenvectors should satisfy

$$\langle 1|\rho\rangle = 1, \quad \langle y_j|x_k\rangle = \delta_{j,k}, \quad \text{and} \quad \langle 1|x_j\rangle = \langle y_j|\rho\rangle = 0. \quad (\text{S15})$$

This allows us to write the following operator decompositions:

$$I = |\rho\rangle\langle 1| + \sum_j |x_j\rangle\langle y_j|, \quad (\text{S16})$$

$$\mathcal{L} = \sum_j \lambda_j |x_j\rangle\langle y_j|, \quad (\text{S17})$$

and

$$e^{\mathcal{L}t} = |\rho\rangle\langle 1| + \sum_j e^{\lambda_j t} |x_j\rangle\langle y_j|, \quad (\text{S18})$$

where  $I$  in Eq. (S16) is the identity matrix in the vectorized space. With these definitions, the double integral in Eq. (S12) can now be written as

$$\int_0^\tau dt \int_0^t dt_1 e^{\mathcal{L}(t-t_1)} = \sum_j \left( \frac{e^{\lambda_j \tau} - \lambda_j \tau - 1}{\lambda_j^2} \right) |x_j\rangle\langle y_j| + \frac{\tau^2}{2} |\rho\rangle\langle 1|. \quad (\text{S19})$$

This result holds for arbitrary  $\tau$  and could be useful, for instance, if one wishes to extend the present calculations beyond the asymptotic regime. In our case, however, we are only interested in large  $\tau$ , or, more precisely, in  $\lambda_j \tau \gg 1$  for all  $\lambda_j$ . As a consequence, the integral reduces to

$$\int_0^\tau dt \int_0^t dt_1 e^{\mathcal{L}(t-t_1)} = \frac{\tau^2}{2} |\rho\rangle\langle 1| - \tau \mathcal{L}^+, \quad (\text{S20})$$

where

$$\mathcal{L}^+ = \sum_j \frac{1}{\lambda_j} |x_j\rangle\langle y_j| \quad (\text{S21})$$

is the Drazin inverse of the Liouvillian  $\mathcal{L}$ . Since  $\mathcal{D}$  is traceless, when plugging Eq. (S20) into Eq. (S12), the term proportional to  $\tau^2$  vanishes, and we obtain

$$\partial_\theta \text{E}_\theta[N(\tau)]_{\theta=0} = \tau J - \tau \sum_k \nu_k \text{Tr}\{\hat{L}_k^\dagger \hat{L}_k \mathcal{L}^+ \mathcal{D} \hat{\rho}_0\}. \quad (\text{S22})$$

Finally, using the facts that  $\mathcal{L} = \mathcal{H} + \mathcal{D}$  and that  $\hat{\rho}_0$  is the steady state  $\hat{\rho}_{\text{ss}}$ , we obtain

$$\partial_\theta \text{E}_\theta[N(\tau)]_{\theta=0} = \tau J (1 + \psi), \quad (\text{S23})$$

where the factor  $\psi$  is given by Eq. (6) in the main text, reproduced here for convenience:

$$\psi = \frac{1}{J} \text{Tr}\{\mathcal{J} \mathcal{L}^+ \mathcal{H} \hat{\rho}_{\text{ss}}\}. \quad (\text{S24})$$

Here we have employed the current superoperator,  $\mathcal{J} \hat{\rho} = \sum_k \nu_k L_k \hat{\rho} L_k^\dagger$ , see Eq. (7) in the main text.

For a diffusive current, Eq. (S6) takes the form

$$\text{E}_\theta[N(\tau)] = \sqrt{1 + \theta} \int_0^\tau dt \nu_k \text{Tr}\{\mathcal{J}_d e^{\mathcal{L}_d t} \hat{\rho}_0\}. \quad (\text{S25})$$

One can notice that the only difference is the factor in front. As a result, Eq. (S22) becomes

$$\partial_\theta \text{E}_\theta[N(\tau)]_{\theta=0} = \frac{1}{2} \tau J_d - \tau \text{Tr}\{\mathcal{J}_d \mathcal{L}^+ \mathcal{D} \hat{\rho}_0\}, \quad (\text{S26})$$

where we used  $\partial_\theta \sqrt{1 + \theta}|_{\theta=0} = 1/2$ . The remaining calculations remain the same.

## II. Restricting $\psi$ for series of conductances

Here we consider currents that can be written as a series of conductances

$$J = \left( \sum_j \gamma_j + \sum_k W_k \right)^{-1}, \quad (\text{S27})$$

where  $\gamma_j$  are proportional to the rates occurring in the Lindblad jump operators, whereas

$$W_k = \frac{g_k^2}{\Gamma_k}, \quad (\text{S28})$$

are rates that follow from a perturbative treatment of coherent tunneling terms. In Eq. (S28),  $g_k$  is proportional to the coherent tunneling rates, while  $\Gamma_k$  is proportional to the Lindblad jump rates. The deformation used to derive the  $\psi$ -KUR thus results in

$$\gamma_l \rightarrow \gamma_l(1 + \theta), \quad W_k \rightarrow W_k/(1 + \theta) \simeq W_k(1 - \theta), \quad (\text{S29})$$

where the last relation holds for small  $\theta$ . To linear order in  $\theta$ , the deformed integrated current follows from Eqs. (S27) and (S29) as

$$E_\theta[N(\theta)] = J\tau(1 + \theta\alpha), \quad \alpha = \frac{\sum_l \gamma_l^{-1} - \sum_k W_k^{-1}}{\sum_l \gamma_l^{-1} + \sum_k W_k^{-1}}. \quad (\text{S30})$$

Since all the rates are positive,  $-1 \leq \alpha \leq 1$ . From Eq. (S23), we find  $\alpha - 1 = \psi$ , implying that  $-2 \leq \psi \leq 0$ .

## III. Quantum KUR of Ref. [48]

The quantum correction  $\chi$  in the quantum KUR in Eq. (9) is given by [48]

$$\chi = -4 \left( \text{Tr}\{\mathcal{K}_L \mathcal{L}^+ \mathcal{K}_R \hat{\rho}_{\text{ss}}\} + \text{Tr}\{\mathcal{K}_R \mathcal{L}^+ \mathcal{K}_L \hat{\rho}_{\text{ss}}\} \right), \quad (\text{S31})$$

where

$$\begin{aligned} \mathcal{K}_L \hat{\rho} &= -i\hat{H}\hat{\rho} + \frac{1}{2} \sum_k \left( \hat{L}_k \hat{\rho} \hat{L}_k^\dagger - \hat{L}_k^\dagger \hat{L}_k \hat{\rho} \right), \\ \mathcal{K}_R \hat{\rho} &= i\hat{\rho}\hat{H} + \frac{1}{2} \sum_k \left( \hat{L}_k \hat{\rho} \hat{L}_k^\dagger - \hat{\rho} \hat{L}_k^\dagger \hat{L}_k \right). \end{aligned} \quad (\text{S32})$$

## IV. Vectorization and Drazin inverse

### Vectorization

In order to analytically compute fluctuations of currents and the KUR bounds, we express the density matrix of the system,  $\hat{\rho}$ , as a matrix

$$\hat{\rho} = \sum_{i,j} \rho_{ij} |i\rangle\langle j| \quad (\text{S33})$$

in a basis  $\{|i\rangle, |j\rangle\}$  of the Hilbert space and write the Lindblad master equation (3) in the vectorized form [22]:

$$\frac{d}{dt} |\rho\rangle = \mathcal{L} |\rho\rangle, \quad (\text{S34})$$

where  $|\rho\rangle$  is a vectorized density matrix. The vectorization of the density matrix follows a convention of stacking the columns on top of each other such that the first one is on the top, i.e.  $|\rho\rangle = [\rho_{11}, \rho_{21}, \rho_{31}, \dots, \rho_{12}, \rho_{22}, \rho_{32}, \dots]^T$ . The vectorized Liouvillian  $\mathcal{L}$  can be obtained using the following relation for matrices  $M_{1,2}$ :

$$M_1 \hat{\rho} M_2 \rightarrow M_2^T \otimes M_1 |\rho\rangle. \quad (\text{S35})$$

The steady state  $|\rho\rangle$  is the eigenvector of  $\mathcal{L}$  corresponding to the zero eigenvalue. The remaining superoperators that are necessary to compute  $\psi$  such as  $\mathcal{H}$  and  $\mathcal{J}$  can be vectorized using the same technique.

### Drazin inverse

The Drazin inverse  $\mathcal{L}^+$  [65] of the Liouvillian  $\mathcal{L}$  can be found from the Moore-Penrose inverse  $\mathcal{L}^{\text{MP}}$  by projecting away the null space, i.e.,

$$\mathcal{L}^+ = (\hat{I} - \mathcal{P})\mathcal{L}^{\text{MP}}(\hat{I} - \mathcal{P}), \quad (\text{S36})$$

where  $\hat{I}$  is an identity operator and  $\mathcal{P}\bullet := \hat{\rho}_{\text{ss}}\text{Tr}\{\bullet\}$ . The Drazin inverse can be directly computed using the formula

$$\mathcal{L}^+ = -\int_0^\infty ds e^{\mathcal{L}s}(\hat{I} - \mathcal{P}). \quad (\text{S37})$$

In the vectorized notation,  $\mathcal{P}$  becomes  $|\rho\rangle\langle 1|$ , where  $|\rho\rangle$  and  $\langle 1|$  are right and left eigenvectors of  $\mathcal{L}$  corresponding to the zero eigenvalue, respectively. The vectorized Drazin inverse  $\mathcal{L}^+$  applied to a given  $|x\rangle$  can be evaluated as  $\mathcal{L}^+|x\rangle = (I - |\rho\rangle\langle 1|)|y\rangle$ , where  $|y\rangle$  is a solution to  $\mathcal{L}|y\rangle = (I - |\rho\rangle\langle 1|)|x\rangle$ , and  $I$  is a vectorized  $\hat{I}$ .

### Noise $D$

To compute the noise  $D$ , see Eq. (4) in the main text, we may employ a method of full counting statistics [64], which we briefly summarize here. We introduce a counting field  $\chi$  and a generalized master equation

$$\mathcal{L}_\chi \hat{\rho}_t(\chi) \equiv \mathcal{L} \hat{\rho}_t(\chi) + \sum_k (e^{i\nu_k \chi} - 1) \hat{L}_k \hat{\rho}_t(\chi) \hat{L}_k^\dagger, \quad (\text{S38})$$

where  $\mathcal{L}$  is the Liouvillian, see Eq. (3) in the main text. For the initial state  $\hat{\rho}_0$  that is assumed to be the steady state of  $\mathcal{L}$ , a formal solution is given by  $\hat{\rho}_t(\chi) = e^{\mathcal{L}_\chi t} \hat{\rho}_0$ . In the long time limit, the average current  $J$  and the noise  $D$  are given by

$$J = -i\partial_\chi \lambda(\chi)|_{\chi=0}, \quad D = -\partial_\chi^2 \lambda(\chi)|_{\chi=0}, \quad (\text{S39})$$

where  $\lambda(\chi)$  is the eigenvalue of  $\mathcal{L}_\chi$  with a largest real part.

The noise  $D$  for the quantum jump unravelling can be explicitly evaluated using the expression [22]

$$D = \sum_k \text{Tr}\{\nu_k^2 \hat{L}_k \hat{\rho} \hat{L}_k^\dagger\} - 2\text{Tr}\{\mathcal{J} \mathcal{L}^+ \mathcal{J} \hat{\rho}\}. \quad (\text{S40})$$

For the diffusive unravelling,  $D$  can be obtained using the formula [22]

$$D = \sum_k \nu_k^2 - 2\text{Tr}\{\mathcal{J}_d \mathcal{L}^+ \mathcal{J}_d \hat{\rho}\}. \quad (\text{S41})$$

## V. Double quantum dot

### Time evolution and density matrix

Fluctuations of the electron current passing through the DQD have been investigated recently [4]. Using the basis  $\{|n_L, n_R\rangle \equiv (\hat{c}_L^\dagger)^{n_L} (\hat{c}_R^\dagger)^{n_R} |0, 0\rangle\}$ , which corresponds to the occupation of each quantum dot, the steady-state density matrix has the following form:

$$\hat{\rho} = \begin{pmatrix} p_0 & 0 & 0 & 0 \\ 0 & p_L & \alpha & 0 \\ 0 & \alpha^* & p_R & 0 \\ 0 & 0 & 0 & p_D \end{pmatrix}. \quad (\text{S42})$$

The expression for the vectorized Liouvillian corresponding to Eq. (11) in the main text, written in the coefficient basis  $\{p_0, p_L, p_R, p_D, \text{Re}[\alpha], \text{Im}[\alpha]\}$ , reads

$$\mathcal{L} = \begin{pmatrix} -f_L\gamma_L - f_R\gamma_R & (1-f_L)\gamma_L & (1-f_R)\gamma_R & 0 & 0 & 0 \\ f_L\gamma_L & -(1-f_L)\gamma_L - f_R\gamma_R & 0 & (1-f_R)\gamma_R & 0 & -2g \\ f_R\gamma_R & 0 & -f_L\gamma_L - (1-f_R)\gamma_R & (1-f_L)\gamma_L & 0 & 2g \\ 0 & f_R\gamma_R & f_L\gamma_L & -(1-f_L)\gamma_L - (1-f_R)\gamma_R & 0 & 0 \\ 0 & 0 & 0 & 0 & -\frac{\gamma_L+\gamma_R+2\Gamma}{2} & 0 \\ 0 & g & -g & 0 & 0 & -\frac{\gamma_L+\gamma_R+2\Gamma}{2} \end{pmatrix}. \quad (\text{S43})$$

The corresponding steady state is given by

$$\begin{aligned} p_0 &= \frac{4g^2(1-\bar{f})^2(\gamma_L + \gamma_R) + (1-f_L)(1-f_R)\gamma_L\gamma_R(\gamma_L + \gamma_R + 2\Gamma)}{4g^2(\gamma_L + \gamma_R) + \gamma_L\gamma_R(\gamma_L + \gamma_R + 2\Gamma)}, \\ p_D &= \frac{4g^2\bar{f}^2(\gamma_L + \gamma_R) + f_L f_R \gamma_L \gamma_R (\gamma_L + \gamma_R + 2\Gamma)}{4g^2(\gamma_L + \gamma_R) + \gamma_L\gamma_R(\gamma_L + \gamma_R + 2\Gamma)}, \\ p_L &= \frac{4g^2\bar{f}(1-\bar{f})(\gamma_L + \gamma_R) + f_L(1-f_R)\gamma_L\gamma_R(\gamma_L + \gamma_R + 2\Gamma)}{4g^2(\gamma_L + \gamma_R) + \gamma_L\gamma_R(\gamma_L + \gamma_R + 2\Gamma)}, \\ p_R &= \frac{4g^2\bar{f}(1-\bar{f})(\gamma_L + \gamma_R) + (1-f_L)f_R\gamma_L\gamma_R(\gamma_L + \gamma_R + 2\Gamma)}{4g^2(\gamma_L + \gamma_R) + \gamma_L\gamma_R(\gamma_L + \gamma_R + 2\Gamma)}, \\ \alpha &= \frac{2ig(f_L - f_R)\gamma_L\gamma_R}{4g^2(\gamma_L + \gamma_R) + \gamma_L\gamma_R(\gamma_L + \gamma_R + 2\Gamma)}, \end{aligned} \quad (\text{S44})$$

where  $\bar{f} \equiv \frac{f_L\gamma_L + f_R\gamma_R}{\gamma_L + \gamma_R}$ . The  $l_1$  norm of coherence [67] in the occupation basis is defined as  $\mathcal{C} = |\alpha|$ .

### Jump unravelling

We consider a current passing through the DQD, which corresponds to, for instance, setting the weight associated with  $\hat{c}_L^\dagger$  to  $\nu = 1$ , the weight associated with  $\hat{c}_L$  to  $\nu = -1$ , and all remaining weights to  $\nu = 0$ . The average value of the current  $J = \gamma_L \text{Tr}\{f_L \hat{c}_L^\dagger \hat{\rho} \hat{c}_L - (1-f_L) \hat{c}_L \hat{\rho} \hat{c}_L^\dagger\}$  is given by

$$J = \frac{4g^2(f_L - f_R)\gamma_L\gamma_R}{4g^2(\gamma_L + \gamma_R) + \gamma_L\gamma_R(\gamma_L + \gamma_R + 2\Gamma)}. \quad (\text{S45})$$

The dynamical activity reads

$$A = \frac{8g^2(\gamma_L + \gamma_R)^2\bar{f}(1-\bar{f} + \Gamma/(\gamma_L + \gamma_R)) + \gamma_L\gamma_R(\gamma_L + \gamma_R + 2\Gamma)(2\gamma_L f_L(1-f_L) + 2\gamma_R f_R(1-f_R) + \Gamma(f_L + f_R))}{4g^2(\gamma_L + \gamma_R) + \gamma_L\gamma_R(\gamma_L + \gamma_R + 2\Gamma)}. \quad (\text{S46})$$

The analytical expression obtained for the noise with Eq. (S40) is given by

$$\begin{aligned} D &= \frac{4g^2(f_L + f_R - 2f_L f_R)\gamma_L\gamma_R}{4g^2(\gamma_L + \gamma_R) + \gamma_L\gamma_R(\gamma_L + \gamma_R + 2\Gamma)} + J \frac{32g^2(f_L - f_R)\gamma_L\gamma_R(\gamma_L + \gamma_R + \Gamma)}{(\gamma_L + \gamma_R)(4g^2(\gamma_L + \gamma_R) + \gamma_L\gamma_R(\gamma_L + \gamma_R + 2\Gamma))} \\ &\quad - 2J^2 \frac{4g^2(\gamma_L + \gamma_R)(5\gamma_L + 5\gamma_R + 6\Gamma) + 2(\gamma_L + \gamma_R + 2\Gamma)(2\Gamma(\gamma_L^2 + 3\gamma_L\gamma_R + \gamma_R^2) + (\gamma_L + \gamma_R)(\gamma_L^2 + 7\gamma_L\gamma_R + \gamma_R^2))}{(\gamma_L + \gamma_R)(4g^2(\gamma_L + \gamma_R) + \gamma_L\gamma_R(\gamma_L + \gamma_R + 2\Gamma))}. \end{aligned} \quad (\text{S47})$$

### Diffusive unravelling

For the diffusive unravelling, the average current  $J_d = \sqrt{2\Gamma} \text{Tr}\{(\hat{c}_L^\dagger \hat{c}_L - \hat{c}_R^\dagger \hat{c}_R) \hat{\rho}\}$  is given by

$$J_d = \frac{\sqrt{2\Gamma}(f_L - f_R)\gamma_L\gamma_R(\gamma_L + \gamma_R + 2\Gamma)}{4g^2(\gamma_L + \gamma_R) + \gamma_L\gamma_R(\gamma_L + \gamma_R + 2\Gamma)}, \quad (\text{S48})$$

and the dynamical activity is still given in Eq. (S46). The expression for the noise  $D$ , which is computed using Eq. (S41) and Eq. (8) in the main text, with  $\nu = 1$ ,  $\phi = 0$ , and  $\hat{L} = \hat{c}_L^\dagger \hat{c}_L - \hat{c}_R^\dagger \hat{c}_R$ , is omitted here due to its length.

### Factor $\psi$ for unidirectional counting

In the case of the jump unravelling, if we count only electrons entering the system from the left reservoir, which corresponds to the current  $J = \gamma_L f_L \text{Tr}\{\hat{c}_L^\dagger \hat{\rho} \hat{c}_L\}$ , we find the factor  $\psi$ , without dephasing for simplicity ( $\Gamma = 0$ ):

$$\psi = \frac{8g^2(f_L - f_R)\gamma_L\gamma_R^2}{(4g^2 + \gamma_L\gamma_R)((f_L - 1)\gamma_L\gamma_R(\gamma_L + \gamma_R) + 4g^2((f_L - 1)\gamma_L + (f_R - 1)\gamma_R))}, \quad (\text{S49})$$

which can be positive.

## VI. Effective classical model of the double quantum dot

### Rate equation

The time evolution of the vector of populations  $\vec{p} = [p_0, p_L, p_R, p_D]^T$  in the classical model given in Eq. (15) in the main text is described by the transition matrix

$$W = \begin{pmatrix} -f_L\gamma_L - f_R\gamma_R & (1 - f_L)\gamma_L & (1 - f_R)\gamma_R & 0 \\ f_L\gamma_L & -(1 - f_L)\gamma_L - f_R\gamma_R - W_{RL} & W_{LR} & (1 - f_R)\gamma_R \\ f_R\gamma_R & W_{RL} & -f_L\gamma_L - (1 - f_R)\gamma_R - W_{LR} & (1 - f_L)\gamma_L \\ 0 & f_R\gamma_R & f_L\gamma_L & -(1 - f_L)\gamma_L - (1 - f_R)\gamma_R \end{pmatrix}, \quad (\text{S50})$$

where  $W_{LR} = W_{RL} = \frac{4g^2}{\gamma_L + \gamma_R + 2\Gamma}$ , which has already been introduced in Eq. (16) in the main text, replaces the coherent tunneling. The remaining elements of the matrix  $W$ , which correspond to transitions due to the reservoirs, are obtained directly from the dissipative part of the Lindblad master equation (11). The effective classical model captures both the average current  $J$  (S45) across the DQD and the steady state of the quantum model, meaning that the steady state of  $W$  agrees with the diagonal elements of the steady-state density matrix (S44).

The expressions for the noise in the classical model, which is different from the quantum expression (S47), can be found using Eq. (S40) adapted to the classical rate equation:

$$D = \frac{4g^2(f_L + f_R - 2f_L f_R)\gamma_L\gamma_R}{4g^2(\gamma_L + \gamma_R) + \gamma_L\gamma_R(\gamma_L + \gamma_R + 2\Gamma)} + J \frac{16g^2(f_L - f_R)\gamma_L\gamma_R}{4g^2(\gamma_L + \gamma_R) + \gamma_L\gamma_R(\gamma_L + \gamma_R + 2\Gamma)} - 2J^2 \frac{12g^2(\gamma_L + \gamma_R) + (\gamma_L + \gamma_R + 2\Gamma)(\gamma_L^2 + 3\gamma_L\gamma_R + \gamma_R^2)}{(\gamma_L + \gamma_R)(4g^2(\gamma_L + \gamma_R) + \gamma_L\gamma_R(\gamma_L + \gamma_R + 2\Gamma))}, \quad (\text{S51})$$

where  $J$  is given in Eq. (S45). The dynamical activity of the classical model, defined as  $A_{\text{cl}} = \sum_{j \neq k} W_{kj} p_j$ , is given by the expression

$$A_{\text{cl}} = A + \left( \frac{4g^2}{\gamma_L + \gamma_R + 2\Gamma} - \frac{\Gamma}{2} \right) (p_L + p_R), \quad (\text{S52})$$

where  $p_{L,R}$  are provided in Eq. (S44), and  $A$  is the dynamical activity of the quantum model (S46). The term proportional to  $\Gamma$  is subtracted, because dephasing jumps contribute to the dynamical activity in the quantum model, but they do not in the classical rate equation. Hence, for small  $g$  as well as  $\Gamma$ , we have  $A \simeq A_{\text{cl}}$ .

### Adiabatic elimination for large $g$

Increasing the value of  $g$  gives rise to a larger dynamical activity  $A_{\text{cl}}$  due to frequent transitions of electrons between the left and right quantum dots. For large  $g$ , the rate of the interdot transitions is much higher than the rate of the transitions in and out of the system, leading to  $p_L \simeq p_R$ . However, these fast interdot oscillations do not influence fluctuations of the current and are, therefore, redundant in the description of the dynamics of the system. The effective dynamics is described by the three-state model, where we coarse-grain the states with a single electron occupation, resulting in the rate equation for the vector  $\vec{p} = [p_0, p_L + p_R, p_D]$ . The associated transition matrix is obtained using the adiabatic elimination as follows. First, we make a basis change  $\vec{p} = [p_0, p_L, p_R, p_D] \rightarrow \vec{p} = [p_0, p_L + p_R, p_L - p_R, p_D]$ .

The corresponding transition matrix reads

$$\tilde{W} = \begin{pmatrix} -f_L\gamma_L - f_R\gamma_R & \frac{(1-f_L)\gamma_L + (1-f_R)\gamma_R}{2} & \frac{(1-f_L)\gamma_L - (1-f_R)\gamma_R}{2} & 0 \\ f_L\gamma_L + f_R\gamma_R & -\frac{\gamma_L + \gamma_R}{2} & -\frac{\gamma_L(1-2f_L) + \gamma_R(1-2f_R)}{2} & (1-f_L)\gamma_L + (1-f_R)\gamma_R \\ f_L\gamma_L - f_R\gamma_R & -\frac{\gamma_L(1-2f_L) + \gamma_R(1-2f_R)}{2} & -\frac{\gamma_L + \gamma_R + 4W_{LR}}{2} & -(1-f_L)\gamma_L + (1-f_R)\gamma_R \\ 0 & \frac{f_L\gamma_L + f_R\gamma_R}{2} & -\frac{f_L\gamma_L + f_R\gamma_R}{2} & -(1-f_L)\gamma_L - (1-f_R)\gamma_R \end{pmatrix}. \quad (\text{S53})$$

Let  $+$  and  $-$  denote the states corresponding to  $p_L + p_R$  and  $p_L - p_R$ , respectively. In the steady state, the expression for  $p_-$  reads  $p_- = -(\tilde{W}_{-0}p_0 + \tilde{W}_{-+}p_+ + \tilde{W}_{-D}p_D)/\tilde{W}_{--}$ . We may insert it into each equation  $\frac{d}{dt}p_k = \sum_{j \in \{0,+,D\}} \tilde{W}_{kj}p_j + \tilde{W}_{k-}p_-$  describing the time evolution of the probabilities  $p_k$  for  $k \in \{0,+,D\}$ , which results in a coupled system of differential equations for  $p_{0,+,D}$ . It can be expressed as a new rate equation  $\frac{d}{dt}\vec{p} = \mathbb{W}\vec{p}$ , with  $\vec{p} = [p_0, p_+, p_D]$ , where

$$\mathbb{W}_{kj} = \tilde{W}_{kj} - \frac{\tilde{W}_{k-}\tilde{W}_{-j}}{\tilde{W}_{--}}. \quad (\text{S54})$$

The corresponding dynamical activity is given by  $A_{\text{ad}} = \sum_{k,j \in \{0,+,D\}: k \neq j} \mathbb{W}_{kj}p_j$ , resulting in

$$A_{\text{ad}} = (\gamma_L + \gamma_R) \frac{128g^4\bar{f}(1-\bar{f}) + g^2\mathbb{P}_2 + \mathbb{P}_4}{(4g^2 + \gamma_L\gamma_R)(16g^2 + (\gamma_L + \gamma_R)^2)}, \quad (\text{S55})$$

where  $\mathbb{P}_{2,4}$  are two different polynomials in  $\gamma_L$  and  $\gamma_R$  (with products of  $f_L$  and  $f_R$  being coefficients) of the order 2 and 4, respectively. Therefore, for large  $g/\gamma_{L,R}$ ,  $A_{\text{ad}}$  reduces to  $A_{\text{ad}} \simeq 2(\gamma_L + \gamma_R)\bar{f}(1-\bar{f})$ , which tends to  $A$  in the same limit and small  $\Gamma$ , cf. Eq. (S46).

## VII. Random network of states

We consider a 5-level quantum system in the basis  $\{|n\rangle\}$ . The Hamiltonian of the system is given by

$$\hat{H} = \sum_{n \neq k} g_{nk} |n\rangle\langle k|. \quad (\text{S56})$$

Each transition  $n \leftrightarrow k$  is coherently connected with 50% probability. For each connected transition, values of  $g_{nk} = g_{kn}$  are sampled from a uniform distribution  $U[0, 3]$  with a probability density

$$p_{U[a,b]}(x) = \begin{cases} \frac{1}{b-a} & \text{for } a \leq x \leq b, \\ 0 & \text{otherwise.} \end{cases} \quad (\text{S57})$$

In the case of no coherent transition, we set  $g_{nk} = 0$ , and this connection is mediated by a reservoir-like transition, giving rise to the  $\gamma_{nk}\mathcal{D}[|n\rangle\langle k|] + \gamma_{kn}\mathcal{D}[|k\rangle\langle n|]$  contribution in the Lindblad master equation of the system. Each  $\gamma_{nk}$  is sampled from  $U[0, 3]$ , whereas  $\gamma_{kn} = \gamma_{nk}e^{-\sigma_{nk}}$ , where  $\sigma_{nk}$  is sampled from  $U[3, 5]$  to ensure a strong bias. Current is calculated along a single reservoir-like transition with antisymmetric weights,  $J = \gamma_{10}\langle 0|\hat{\rho}_{\text{ss}}|0\rangle - \gamma_{01}\langle 1|\hat{\rho}_{\text{ss}}|1\rangle$ . We simulated 1000 random network configurations and computed  $J, D, A, \psi$ , and  $\chi$  for each of them. The scatter plot of  $DA/J^2$  against  $(1 + \psi)^2$  (red circles) and against  $A/(A + \chi)$  (green circles) is shown in Fig. 2 in the main text.

## VIII. Further example: coherently driven qubit

To further illustrate our results, we investigate a coherently driven qubit with Hamiltonian

$$\hat{H} = \frac{\Delta}{2}\hat{\sigma}_z + \Omega\hat{\sigma}_x, \quad (\text{S58})$$

where  $\Delta$  is the detuning,  $\Omega$  the Rabi frequency, and  $\hat{\sigma}_{x,y,z}$  are Pauli matrices. The qubit is weakly coupled to a thermal reservoir, and its time evolution in the rotating frame may be described by the Liouvillian

$$\partial_t\hat{\rho} = \mathcal{L}\hat{\rho} = -i[\hat{H}, \hat{\rho}] + \kappa\bar{n}D[\hat{\sigma}_+]\hat{\rho} + \kappa(\bar{n} + 1)D[\hat{\sigma}_-]\hat{\rho} \quad (\text{S59})$$



where  $\bar{n} \equiv (\exp(\beta\omega) - 1)^{-1}$  denotes the Bose-Einstein occupation,  $\beta$  is the inverse temperature of the reservoir,  $\kappa$  is the strength of the coupling to the reservoir, and  $\omega$  is the energy gap of the qubit in the Schrödinger picture.

The Hamiltonian (S58) may be implemented with a two-level atom characterized by a transition frequency  $\omega$  and driven by a coherent laser field with a frequency  $\omega_d$ . The corresponding time-dependent Hamiltonian  $\hat{H}(t) = \hat{H}_0 + \hat{V}(t)$  consists of a bare part,  $\hat{H}_0 = \omega\hat{\sigma}_+\hat{\sigma}_-$ , and a driving contribution,  $\hat{V}(t) = \Omega(\hat{\sigma}_+ \exp(-i\omega_d t) + \hat{\sigma}_- \exp(i\omega_d t))$ , where  $\hat{\sigma}_\pm = (\hat{\sigma}_x \pm i\hat{\sigma}_y)/2$  is a raising (lowering) operator. Upon moving to the rotating frame with respect to  $\exp(i\omega_d t\hat{\sigma}_+\hat{\sigma}_-)$ , we obtain the Hamiltonian in Eq. (S58), where the detuning is given by  $\Delta = \omega - \omega_d$ .

In the basis  $\{|0\rangle, |1\rangle\}$ , which corresponds to, respectively, the ground and the excited state, the steady-state density matrix can be written as

$$\hat{\rho} = \begin{pmatrix} \rho_{00} & \rho_{01} \\ \rho_{10} & \rho_{11} \end{pmatrix}. \quad (\text{S60})$$

The vectorized Liouvillian (S59) expressed in the coefficient basis  $\{\rho_{00}, \rho_{10}, \rho_{01}, \rho_{11}\}$  is given by

$$\mathcal{L} = \begin{pmatrix} -\kappa\bar{n} & -i\Omega & i\Omega & \kappa(\bar{n}+1) \\ -i\Omega & -i\Delta - \kappa(2\bar{n}+1)/2 & 0 & i\Omega \\ i\Omega & 0 & i\Delta - \kappa(2\bar{n}+1)/2 & -i\Omega \\ \kappa\bar{n} & i\Omega & -i\Omega & -\kappa(\bar{n}+1) \end{pmatrix}. \quad (\text{S61})$$

The corresponding steady-state solution reads

$$\begin{aligned} \rho_{00} &= \frac{(1 + \bar{n})(\mathcal{Q} - 8\Omega^2) + 4(1 + 2\bar{n})\Omega^2}{(1 + 2\bar{n})\mathcal{Q}}, \\ \rho_{10} &= \frac{2(-i\kappa(1 + 2\bar{n}) - 2\Delta)\Omega}{(1 + 2\bar{n})\mathcal{Q}}, \\ \rho_{01} &= \frac{2(i\kappa(1 + 2\bar{n}) - 2\Delta)\Omega}{(1 + 2\bar{n})\mathcal{Q}}, \\ \rho_{11} &= \frac{\bar{n}(\mathcal{Q} - 8\Omega^2) + 4(1 + 2\bar{n})\Omega^2}{(1 + 2\bar{n})\mathcal{Q}}, \end{aligned} \quad (\text{S62})$$

where  $\mathcal{Q} = \kappa^2(1 + 2\bar{n})^2 + 4(\Delta^2 + 2\Omega^2)$ .

### Jump current

We consider the average current passing from the qubit to the reservoir, which corresponds to setting  $\nu = 1$  for  $\hat{\sigma}_-$  and  $\nu = -1$  for  $\hat{\sigma}_+$ , i.e.,

$$\mathcal{J}\hat{\rho}_{ss} = \kappa(\bar{n} + 1)\hat{\sigma}_-\hat{\rho}_{ss}\hat{\sigma}_-^\dagger - \kappa\bar{n}\hat{\sigma}_+\hat{\rho}_{ss}\hat{\sigma}_+^\dagger. \quad (\text{S63})$$

The analytical expression is given by

$$J = \frac{4\kappa\Omega^2}{\mathcal{Q}}. \quad (\text{S64})$$

The dynamical activity of the qubit is given by the compact expression  $A = \kappa\bar{n}\rho_{00} + \kappa(\bar{n} + 1)\rho_{11}$ . Inserting the steady-state solution (S62) leads to

$$A = \frac{2\kappa\bar{n}(1 + \bar{n})(\mathcal{Q} - 8\Omega^2) + 4\kappa(1 + 2\bar{n})^2\Omega^2}{(1 + 2\bar{n})\mathcal{Q}}. \quad (\text{S65})$$

The noise  $D$  evaluated with Eq. (S40) is given by

$$D = A + \frac{2\kappa \left( \bar{n}(1 + \bar{n})(\mathcal{Q} - 8\Omega^2)^3 + 16\bar{n}(1 + \bar{n})(\mathcal{Q} - 8\Omega^2)^2\Omega^2 + 16(\kappa^2(1 + 2\bar{n})^2(3 + 4\bar{n}(1 + \bar{n})) + 4(-1 + 4\bar{n}(1 + \bar{n}))\Delta^2)\Omega^4 \right)}{(1 + 2\bar{n})\mathcal{Q}^3}. \quad (\text{S66})$$

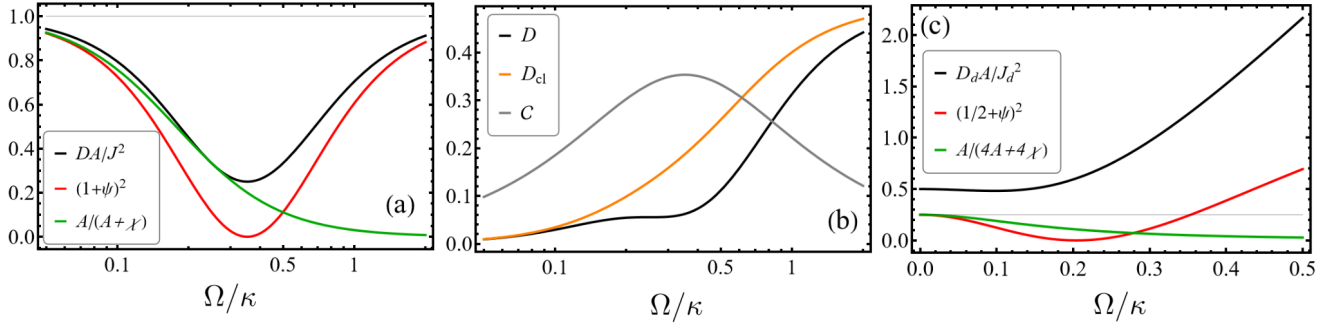


FIG. S1. Quantum KUR in the coherently driven qubit. (a) Quantum jump unravelling:  $DA/J^2$  (black),  $(1+\psi)^2$  bound of the  $\psi$ -KUR (2) (red) obtained with Eq. (S67), and  $A/(A+\chi)$  bound of the KUR (9). Parameters:  $\bar{n} = 0$  and  $\Delta = 0$ . (b) The noise  $D$  for quantum model (S59) (black) and the classical model (S68) (orange), and  $l_1$  norm of coherence  $C$  with parameters of (a). (c) Diffusive unravelling: analogous plots as in (a) for the diffusive measurement of the current in Eq. (S70). Parameters are the same as in (a).

The expression for the factor  $\psi$  (6) reads

$$\psi = \frac{-2\kappa^2(1+2\bar{n})^2}{Q}. \quad (\text{S67})$$

The  $\psi$ -KUR (2) is illustrated in Fig. S1(a), where we show  $(1+\psi)^2$  (red line) bounding the ratio  $DA/J^2$  (black line) from below and compare with the  $A/(A+\chi)$  (green line). The observation made in the main text for the DQD that the dips in  $(1+\psi)^2$  and  $DA/J^2$  coincide carries over to the coherently driven qubit. We also show the  $l_1$  norm of coherence,  $C = (|\rho_{01}| + |\rho_{10}|)/2$ , in Fig. S1(b) as the gray line, whose peak appears in the same regime as the forementioned dips.

### Classical model

Similarly to the DQD, we may consider the effective classical model governing the time-evolution of the populations  $\vec{p} = [\rho_{00}, \rho_{11}]^T$  with a rate equation  $\frac{d}{dt}\vec{p} = W\vec{p}$ . The transition matrix for the qubit system is given by

$$W = \begin{pmatrix} -\kappa\bar{n} - \Gamma_c & \kappa(\bar{n}+1) + \Gamma_c \\ \kappa\bar{n} + \Gamma_c & -\kappa(\bar{n}+1) - \Gamma_c \end{pmatrix}, \quad (\text{S68})$$

where  $\Gamma_c = \frac{4\kappa(1+2\bar{n})\Omega^2}{\kappa^2(1+2\bar{n})^2 + 4\Delta^2}$ . The steady state of the transition matrix  $W$  and the average current  $J$  are the same as the steady-state populations of the quantum model (S62) and the current in Eq. (S64), respectively. The noise  $D$ , however, is different than in the quantum model:

$$D = \frac{4\kappa\Omega^2 \left( (\kappa^2(1+2\bar{n})^3 + 4(1+2\bar{n})\Delta^2)^2 + 8(1+8\bar{n}(1+\bar{n}))(\kappa^2(1+2\bar{n})^2 + 4\Delta^2)\Omega^2 + 64(1+2\bar{n})^2\Omega^4 \right)}{(1+2\bar{n})Q^3}. \quad (\text{S69})$$

Like in the DQD case, there is a regime where  $D$  of the classical rate equation fails to capture  $D$  of the quantum model, which is illustrated in Fig. S1(b). This regime coincides with the regime where  $DA/J^2$  and  $(1+\psi)^2$  display dips in Fig. S1(a). This implies that likewise, for the coherently driven qubit,  $\psi$  indicates a contributing role of coherence to overcoming the classical bound when the effective classical model is insufficient to describe the noise faithfully. Away from this regime, where the classical model provides a faithful description of  $D$ , the factor  $(1+\psi)^2$  approaches 1.

### Diffusive current

For the diffusive current we consider  $\phi = \pi/2$  in Eq. (8) in the main text, resulting in

$$\mathcal{J}_d \hat{\rho}_{ss} = \kappa(\bar{n}+1) \left( -i\hat{\sigma}_- \hat{\rho}_{ss} + i\hat{\rho}_{ss} \hat{\sigma}_-^\dagger \right) - \kappa\bar{n} \left( -i\hat{\sigma}_+ \hat{\rho}_{ss} + i\hat{\rho}_{ss} \hat{\sigma}_+^\dagger \right). \quad (\text{S70})$$

The expression for the current reads

$$J_d = 4\kappa\Omega \frac{\sqrt{\kappa\bar{n}} + \sqrt{\kappa(1+\bar{n})}}{\kappa^2(1+2\bar{n})^2 + 4(\Delta^2 + 2\Omega^2)}. \quad (\text{S71})$$

We omit an explicit analytical expression for  $D$  due to its complexity. We find

$$\psi = \frac{\mathcal{Q} - 2\kappa^2(1+2\bar{n})^2}{\mathcal{Q}}. \quad (\text{S72})$$

The KUR for the diffusive current is illustrated in Fig. S1(c), and the same conclusions as in the case of the DQD can be drawn.